第 29 卷 第 4 期
2003 年 7 月

自 动 化 学 报
ACTA AUTOMATICA SINICA

Vol. 29, No. 4
July, 2003

Restoring Turbulence-Degraded Images Based on Estimation of Turbulence Point Spread Function Values[1)]

ZHANG Tian-Xu HONG Han-Yu SUN Xiang-Hua SONG Zhi

(*Institute for Pattern Recognition and AI, State Key Laboratory of Image Processing and Intelligent Control, Huazhong University of Science and Technology, Wuhan* 430074)

(E-mail: txzhang@mail.hust.edu.cn, honghany@public.wh.hb.cn)

Abstract A new method is proposed for estimating the PSF(point spread function) values of turbulence from turbulence-degraded images. Instead of previously used natural or artificial guide star images to measure the PSF, two consecutive frames of short-exposure turbulence-degraded images are used directly as the input. Appropriate extension are made for the images in the spatial domain and a series of equations for calculating the PSF values are developed and chosen in the frequency domain. In order to overcome the interference of noise, the PSF calculation is transformed into the optimization estimation under the constraints of the PSF being non-negative and spatial smoothing. The values of the PSF are estimated by minimization criteria function and then the degraded images are restored. Experimental results show that the proposed method is highly effective with good performance.

Key words Image restoration, turbulence, PSF, spatial correlation, optimization estimation

1 Introduction

Imaging of objects through atmospheric turbulence is inevitably encountered by space-based, earth-based and plane borne optic imaging sensors working in the turbulence atmospheric environment such as those used in astronomical observation, satellite sensing, precise missile guidance and so on. Owing to the existence of the atmosphere, before light rays enter the window of an imaging sensor, the atmospheric turbulence will randomly interfere with the transmission of the light wave, causing distribution of pixel intensity on the focal plane diffused, peak value reduced, and image blurred. A lot of research has been done to overcome the interference by atmosphere and reconstruct distorted images, and many methods have been proposed for the restoration of turbulence-degraded images. However, none of the methods are free from limitations. For instance, Labeyrie method[1], Knox-Thompson method[2] and the triple correlation method[3] all require a reference star adjacent to the object to detect the PSF. The adaptive optical method[4] can be used to correct the distortion in real-time, but complicated equipment is involved. The blind deconvolution method[5] has been proposed to estimate the intensity of an object using some rational a priori knowledge without a reference guide star , but it excessively depends on a priori knowledge and is mostly handled in an off-line manner[6~8].

To quickly restore images, B. R. Frieden[9] decomposed the influence of the atmospheric turbulence on light wave into a series of optical turbulence units and modeled the atmospheric turbulence PSF as the process of stochastic superposition of a series of disturbance functions (or speckle functions). The Fourier frequency spectra of two consecutive frames of short-exposure images were used to set up the weights and displacements of the "speckle functions", to calculate the PSF . But current solutions are all based on the assumption that the number of turbulence units remain unchanged and the parameters of the basic perturbation function are not changed. In reality, such assumptions are not very ef-

1) Supported by National Natural Science Foundation of P. R. China(60135020) and partily by China-France PRA (SI01-03)

Received May 17, 2002; in revised form December 5, 2002

收稿日期 2002-05-17; 收修改稿日期 2002-12-05

fective; furthermore, the number of the turbulence units is hardly correctly estimated from the turbulence-degraded images.

We propose a new algorithm for recovering turbulence-degraded images based on estimation of the turbulence PSF values. We look at the influence of stochastic turbulence on the imaging of objects from the perspective of the whole, and divide the PSF region into excited and non-excited regions. To avoid the interference of noise, an optimization method to estimate the PSF values based on non-negative and smoothing constraints is suggested, which considerably improves the noise-resisting ability.

2 Equations for calculating the point spread function (PSF)

The 2-D image forming process can be modeled as:

$$g(x,y) = \int_{-\infty}^{\infty}\int_{-\infty}^{\infty} o(x,y)h(x,y;s,t)\mathrm{d}s\mathrm{d}t + \eta(x,y) \tag{1}$$

where $g(x,y)$ represents the observed degraded image, $o(x,y)$ the unknown original image, $\eta(x,y)$ the noise term and $h(x,y;s,t)$ the blurring operator, or PSF.

For a turbulence-degraded image, the process of degradation can in general be assumed to be spatially invariant[10], that is, the blurring operator is uniform across the image. Then we have $h(x,y;k,l)=h(x-k,y-l)$. By substituting it into (1), the turbulence-degraded image $g_n(x,y)$ can be expressed in a convolution form as

$$g_n(x,y) = h_n(x,y) * o(x,y) + \eta_n(x,y) \tag{2}$$

where $h_n(x,y)$ represents the stochastic PSF affected by atmospheric turbulence, $\eta_n(x,y)$ is assumed to be Gaussian additive white noise and the subscript n represents the sequential number of frames of images ($n=1,2,\cdots$).

2.1 Constructing equations

We shall use two consecutive frames of short-exposure turbulence-degraded images $g_n(x,y)(n=1,2)$ of the same object to remove the blur. The two consecutively taken frames can be considered as the degraded images obtained owing to the interference by two stochastically distributed and relatively independent turbulence[11]. According to (2), we perform 2-D DFT for $g_n(x,y)$ $(n=1,2)$, respectively. There will be

$$G_1(u,v) = H_1(u,v)O(u,v) + N_1(u,v) \quad u,v = 0,1,\cdots,N-1 \tag{3}$$

$$G_2(u,v) = H_2(u,v)O(u,v) + N_2(u,v) \quad u,v = 0,1,\cdots,N-1 \tag{4}$$

The frequency spectrum $O(u,v)$ of the original image is unknown. Move $N_1(u,v)$ and $N_2(u,v)$ to the left and divide the Fourier frequency spectrum of (3) by that of (4) and we have

$$D(u,v) = \frac{G_1(u,v)-N_1(u,v)}{G_2(u,v)-N_2(u,v)} = \frac{H_1(u,v)O(u,v)}{H_2(u,v)O(u,v)} = \frac{H_1(u,v)}{H_2(u,v)} \quad u,v = 0,1,\cdots,\mathrm{N}-1 \tag{5}$$

where

$$H_n(u,v) = \sum_{x=0}^{N-1}\sum_{y=0}^{N-1} h_n(x,y)\exp[-j2\pi(ux+vy)/N] \quad n=1,2 \quad u,v=0,1,\cdots,N-1 \tag{6}$$

Suppose the excited region (non-zero region) of the turbulence PSF $h_n(x,y)$ is $M\times M$. In most cases, M is much smaller than the dimension of the image [10]. Suppose the object region in the original image is $R\times C$. In the turbulence-degraded image $g_n(x,y)$, the region actually occupied by the object is larger than that in the original image, its area is $(R+M-1)\times(C+M-1)$. The image of the scene contains the object and the background. To avoid loss of the object energy, it should be ensured that the entire object is in the plane of the image. Suppose the size of the turbulence-degraded image $g_n(x,y)$ is $W\times H$. It should be guaranteed that $W\geqslant R+M-1$, $H\geqslant C+M-1$. To facilitate calculation and using the FFT, we shall perform appropriate periodical extension of $g_n(x,y)$. Here, in order to fa-

cilitate discussion, we make the extension so that it will become a square matrix of $N\times N$. Performing same periodical extension of $h_n(x,y)$ by $N\times N$, then performing 2-D DFT, we have

$$H_n(u,v)=\sum_{x=0}^{N-1}\sum_{y=0}^{N-1}h_n(x,y)\exp[-j2\pi(ux+vy)/N=\sum_{x=0}^{M-1}\sum_{y=0}^{M-1}h_n(x,y)\exp[-j2\pi(ux+vy)/N]\quad n=1,2$$

$$u,v=0,1,\cdots,N-1 \tag{7}$$

Substitution of (7) into (5) yields

$$D(u,v)=\frac{\sum_{x=0}^{M-1}\sum_{y=0}^{M-1}h_1(x,y)\exp[--j2\pi(ux+uy)/N]}{\sum_{x=0}^{M-1}\sum_{y=0}^{M-1}h_2(x,y)\exp[--j2\pi(ux+uy)/N]}\quad u,v=0,1,\cdots,N-1 \tag{8}$$

Performing transposition and collation with respect to the above equation, we have

$$\sum_{x=0}^{M-1}\sum_{y=0}^{M-1}[h_1(x,y)-D(u,v)h_2(x,y)]\exp[-j2\pi(ux+vy)/N]=0\quad u,v=0,1,\cdots,N-1 \tag{9}$$

Express $D(u,v)$ with the amplitude $M_n(u,v)$ and phase angle $\Phi(u,v)$:

$$D(u,v)=M_n(u,v)\exp[j2\pi\phi(u,v)/N] \tag{10}$$

(9) is a complex equation. Substituting (10) into (9) and expanding the real part and imaginary part, respectively, we obtain a series of real part equations and imaginary part equations as follows:

$$\sum_{x=0}^{M-1}\sum_{y=0}^{M-1}\left(\cos\frac{2\pi}{N}(ux+vy)\right)h_1(x,y)-\sum_{x=0}^{M-1}\sum_{y=0}^{M-1}[M_n(u,v)\cos\frac{2\pi}{N}(\phi(u,v)-ux-vy)]h_2(x,y)=0$$

$$\sum_{x=0}^{M-1}\sum_{y=0}^{M-1}\left(\sin\frac{2\pi}{N}(ux+vy)\right)h_1(x,y)+\sum_{x=0}^{M-1}\sum_{y=0}^{M-1}[M_n(u,v)\sin\frac{2\pi}{N}(\phi(u,v)-ux-vy)]h_2(x,y)=0$$

$$u,v=0,1,\cdots,N-1 \tag{11}$$

The above-mentioned (11) contains a total of $2M^2$ unknown variables $h_1(x,y)$ and $h_2(x,y)(x,y=1,2,\cdots,M)$ while in (11) there are $2N^2$ equations. We have noticed that the image's frequency spectra possess conjugate symmetry in the frequency domain. So, of the $2N^2$ equations, about half coincide. In fact, there are N^2+4 linearly independent equations, about half of $2N^2$. Therefore, if $h_1(x,y)$ and $h_2(x,y)$ are to be accurately solved, it should be ensured that $N^2+4>2M^2$, or $N>\sqrt{2}M$. In addition, in order to be able to use the FFT, we choose N as an integer of 2 to a definite power. In short, choose N so that it will satisfy the following three conditions: (a) $N\geqslant\max(W, H)$, (b) $N>(\text{int})\sqrt{2}M$; (c) $N=2^n$, n being a positive integer.

2.2 Transforming the equation set

(11) is in the form of $A\boldsymbol{x}=\boldsymbol{0}$, which is a homogeneous linear equation set. In order to obtain non-zero solution, it is necessary to transform (11) into the form of $A\boldsymbol{x}=\boldsymbol{b}$. We can move a certain variable which is called the reference variable and its corresponding coefficient from the left side to the right side of equations (11). Divide the two sides of (11) by this variable, and we have a non-homogeneous equation set $A\boldsymbol{x}=\boldsymbol{b}$ of order less one. Solve this equation set and the solution obtained will be the ratios of the values of the PSFs $h_1(x,y)$ and $h_2(x,y)$ $(x,y=0,1,2,\cdots,M-1)$ to the reference variable. If we want to find its exact solution, it is necessary to add a constraint condition. Under the condition of the image energy kept conserved, it is obvious that the sum of the PSF values of each turbulence degraded image to be equal 1.0 can be taken as a constraint. In addition, the reference variable should be rationally chosen. Obviously, its value should not be zero, neither

should it relatively be too small. It can be rationally assumed that the peak value of the PSF appears in its center vicinity. Hence, we can choose the center point ($x_0 = M/2, y_0 = M/2$) variable as the reference variable. Suppose its value $h_1(x_o, y_o)$ is 1.0. Then, (11) can be transformed into the following form:

$$\sum_{\substack{x=0 \\ x\neq x_0}}^{M-1}\sum_{\substack{y=0 \\ y\neq y_0}}^{M-1}\left(\cos\frac{2\pi}{N}(ux+vy)\right)h_1(x,y) - \sum_{x=0}^{M-1}\sum_{y=0}^{M-1}[M_n(u,v)\cos\frac{2\pi}{N}(\phi(u,v)-ux-vy)]h_2(x,y) =$$

$$-\cos\frac{2\pi}{N}(ux_0+vy_0)$$

$$\sum_{\substack{x=0 \\ x\neq x_0}}^{M-1}\sum_{\substack{y=0 \\ y\neq y_0}}^{M-1}(\sin\frac{2\pi}{N}(ux+vy))h_1(x,y) + \sum_{x=0}^{M-1}\sum_{y=0}^{M-1}[M_n(u,v)\sin\frac{2\pi}{N}(\phi(u,v)-ux-vy)]h_2(x,y) =$$

$$-\sin\frac{2\pi}{N}(ux_0+vy_0) \qquad u,v=0,1,\cdots,N-1 \qquad (12)$$

2.3 Selection of the equations

This step is of crucial importance in the correct estimation of the turbulence PSF values and is the key part of the proposed algorithm. To ensure the reliability and robustness of the solution, it is necessary to select $(2M^2-1)$ linearly independent equations from the $2N^2$ equations to form a invertible equation set. We propose the following method to effectively select the equations:

1) First, eliminate some linearly dependent equations.

The Fourier frequency spectra possess conjugate symmetry. Of the $2N^2$ equations, in fact about half are repeated and linearly dependent. It is our method to avert the repeated region in the frequency coordinate (u, v) from left to right and from top to bottom (as shown in Fig. 1) to select $(2M^2-1)$ linearly independent equations.

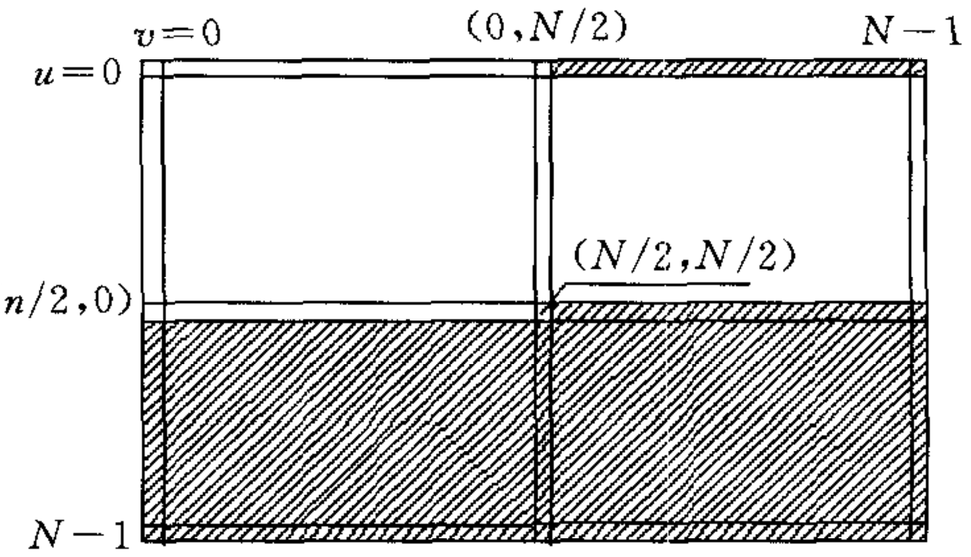

Fig. 1 The repeated region of equations

2) Second, to ensure the stability of the solution, it is necessary to avoid the frequency domain coordinates (u,v) that make $G_n(u,v)(n=1,2)$ equal and close to zero. At the same time, the number of conditions cond(A) should be reduced as much as possible. We adopt the method of quasi-equal spacing (swinging in definite basic spacing) to select equations with definitely different corresponding coefficients from the frequency coordinates uv (shown in Fig. 1). The coefficient matrix A may have perturbation owing to interference of noise while vector $\boldsymbol{b}$ at the right end is accurate and A is in error, which can be expressed as $A+\delta A$. The corresponding solution vector becomes $\boldsymbol{x}+\delta\boldsymbol{x}$. For the number of conditions of non-singular matrix A, $cond(A) = \|A\|\ \|A^{-1}\|$. The relationship between the relative errors of the solution and the matrix coefficient is given in [13] as $\|\delta\boldsymbol{x}\|/\|\boldsymbol{x}+\delta\boldsymbol{x}\| \leqslant \|A^{-1}\|\|\delta A\| = cond(A)\|\delta A\|/\|A\|$. It shows that in order to reduce the relative error of the solution, the number of conditions $cond(A)$ should be as small as possible when the relative error of the coefficient matrix A is controlled within a definite range. Obviously, it should be guaranteed that there exist definite differences in the corresponding coefficient values of the equation variables. To reduce $cond(A)$, we select $(2M^2-1)$ linearly independent equations from the frequency coordinates uv by using quasi-equal spacing.

3) Finally, in the presence of noise, choose as many equations in the low frequency part as possible. In the frequency domain, the energy of the turbulence-degraded image is mainly concentrated in the low frequency part. The values in the low frequencies are great and rather small in the high frequency part while noise is in general distributed in the high

frequency part and the values in the low frequencies are generally rather small. Therefore, if we do not have sufficient a priori knowledge about noise, we should choose as many equations in the low frequency part as possible to prevent the coefficient matrix A from changing too much so that the perturbation of the coefficient matrix δA will be rather small.

2.4 The calculation of the PSF values and direct method

Pick out $(2M^2-1)$ linearly independent equations from equition (12) using the method given in Section 2.3 and make sure that the coefficient matrix is invertible and it's condition number $cond(A)$ is rather small, and then construct the equation set

$$A\boldsymbol{x} = \boldsymbol{b} \tag{13}$$

When there is no noise or only a little noise, $\eta_1(x,y)\approx 0, \eta_2(x,y)\approx 0$. Now $D(u,v)=[G_1(u,v)-N_1(u,v)]/[G_2(u,v)-N_2(u,v)]\approx G_1(u,v)/G_2(u,v)$. Substituting $D(u,v)$ into (5) and solving (13) directly, we have the ratios of PSF values of two turbulence-degraded images to the reference variable. Performing the normalization of the ratios found, we can obtain the discrete values $\hat{h}_1(x,y)$ and $\hat{h}_2(x,y)(x,y=0,1,2,\cdots,M-1)$ with normalized PSF. Performing DFT for $\hat{h}_1(x,y)$ and $\hat{h}_2(x,y)$, respectively, we have $\hat{H}_1(u,v)$ and $\hat{H}_2(u,v)$. The frequency spectra of the original image $\hat{O}_n(u,v)$ can be obtained by inverse filtering, and performing Fourier inversion for $\hat{O}_n(u,v)$ gives the restored images.

3 Optimization estimation based on non-negative and smoothing constraints

In the presence of noise, the errors involved in the turbulence PSF values found by the direct method are too great and the effect of restoration would not be reliable. Now, the noise terms $\eta_1(x,y)$ and $\eta_2(x,y)$ are unpredictable. But we can adopt the non-negative least squares with constraints to estimate the PSF values according to the distribution properties of the degraded images and noise spectra. Let $\hat{D}(u,v)=G_1(u,v)/G_2(u,v)$. The frequency spectra $N_1(u,v)$ and $N_2(u,v)$ of noise are unknown but we have noticed that when $G_1(u,v)$ is much greater than $N_1(u,v)$ and $G_2(u,v)$ is much greater than $N_2(u,v)$, there is $\hat{D}(u,v)\approx D(u,v)$. We use $\hat{D}(u,v)$ to estimate $D(u,v)$. There is $\hat{D}(u,v)\approx D(u,v)$ in the low frequency part. We should choose as many equations as possible in the low frequency part so that the values of the elements of the coefficient matrix of (13) will not change too much and the perturbation will be rather small, that is, $\delta A\approx 0$, and there is $A\boldsymbol{x}\approx\boldsymbol{b}$ as a whole. We shall then constrain the solution according to rational a priori knowledge, and in accordance with some certain criterion, seek the optimal estimate $\hat{\boldsymbol{x}}$ of $\boldsymbol{x}$ to enable $\hat{A}\hat{\boldsymbol{x}}$ to be close to $\boldsymbol{b}$ in the sense of square error. A rational constraint is that the PSF values are greater than or equal to zero, that is, finding the minimum for the following criterion function $\Phi(\boldsymbol{x})$ under non-negative constraint:

$$\hat{\boldsymbol{x}} = \arg\min_{\boldsymbol{x}}\Phi(\boldsymbol{x}) = \arg\min_{\boldsymbol{x}}(A\boldsymbol{x}-\boldsymbol{b})^{\mathrm{T}}(A\boldsymbol{x}-\boldsymbol{b}) \quad \boldsymbol{x}\geqslant 0 \tag{14}$$

The criterion function $\Phi(\boldsymbol{x})$ mentioned above has not any spatial constraint. It allows for great differences among adjacent points and is particularly sensitive to noise. To avoid these latent problems, some penalty terms that can play the role of smoothing must be added to the criterion function (14) according to the spatial correlation to make the difference of PSF values among the adjacent points not too great. The above-mentioned problem can be summed up as the following problem of constraint optimization:

$$\hat{\boldsymbol{x}} = \arg\min_{\boldsymbol{x}}\Phi(\boldsymbol{x}) = \arg\min_{\boldsymbol{x}}\Big[(A\boldsymbol{x}-\boldsymbol{b})^{\mathrm{T}}(A\boldsymbol{x}-\boldsymbol{b}) + \alpha\sum_i P_i(\boldsymbol{x})\Big] \quad \boldsymbol{x}\geqslant 0 \tag{15}$$

where $P_i(\boldsymbol{x})$ is the spatial penalty term of the ith component with respect to $\boldsymbol{x}$, α is a regulating parameter. $P_i(\boldsymbol{x})$ is expressed as follows using the quadratic spatial penalty function:

$$P_i(\boldsymbol{x}) = \sum_j\sum_k w_{jk}(x_{ij}-x_{ik})^2 \tag{16}$$

where w_{jk} of the four most adjacent horizontal and vertical points of the ith component $\boldsymbol{x}_i$ is equal to unity, the remaining being zero.

The optimal solution vector $\hat{\boldsymbol{x}}$ can be obtained by minimizing the criterion function. After transforming the obtained solution vector $\hat{\boldsymbol{x}}$ into discrete values $\hat{h}_1(x,y)$ and $\hat{h}_2(x,y)$ $(x,y=0,1,2,\cdots,M-1)$ and performing normalization respectively, the estimation of the PSF values of the two turbulence-degraded images will be obtained. Performing DFT with respect to $\hat{h}_1(x,y)$ and $\hat{h}_2(x,y)$, we have $\hat{H}_1(u,v)$ and $\hat{H}_2(u,v)$. As the degraded images are polluted by noise, we adopt the filtering method based on the least squares and maximum smoothing criterion described in [12] to estimate the frequency spectrum $\hat{O}_n(u,v)$ $(n=1,2)$ of the original images. Perform IDFT for $\hat{O}_n(u,v)(n=1,2)$ and the restored images can be obtained.

4 Experimental results and analysis

Based on the above-mentioned algorithms, we have developed a simulation software system of the turbulence-degraded images and the restoring software system by programming with VC6.0 on a microprocessor (Pentium III550, 256 mega-memory). By adopting the stochastic superposition model proposed by B. R. Frieden[9], we have generated a series of atmospheric turbulence-degraded images with computer simulation software.

Fig. 2(a) is a satellite cloud image of an area of 130×130. The two stochastically generated original PSFs are as shown in Figs. 2(b) and 2(c). Their excited region is 48×48.

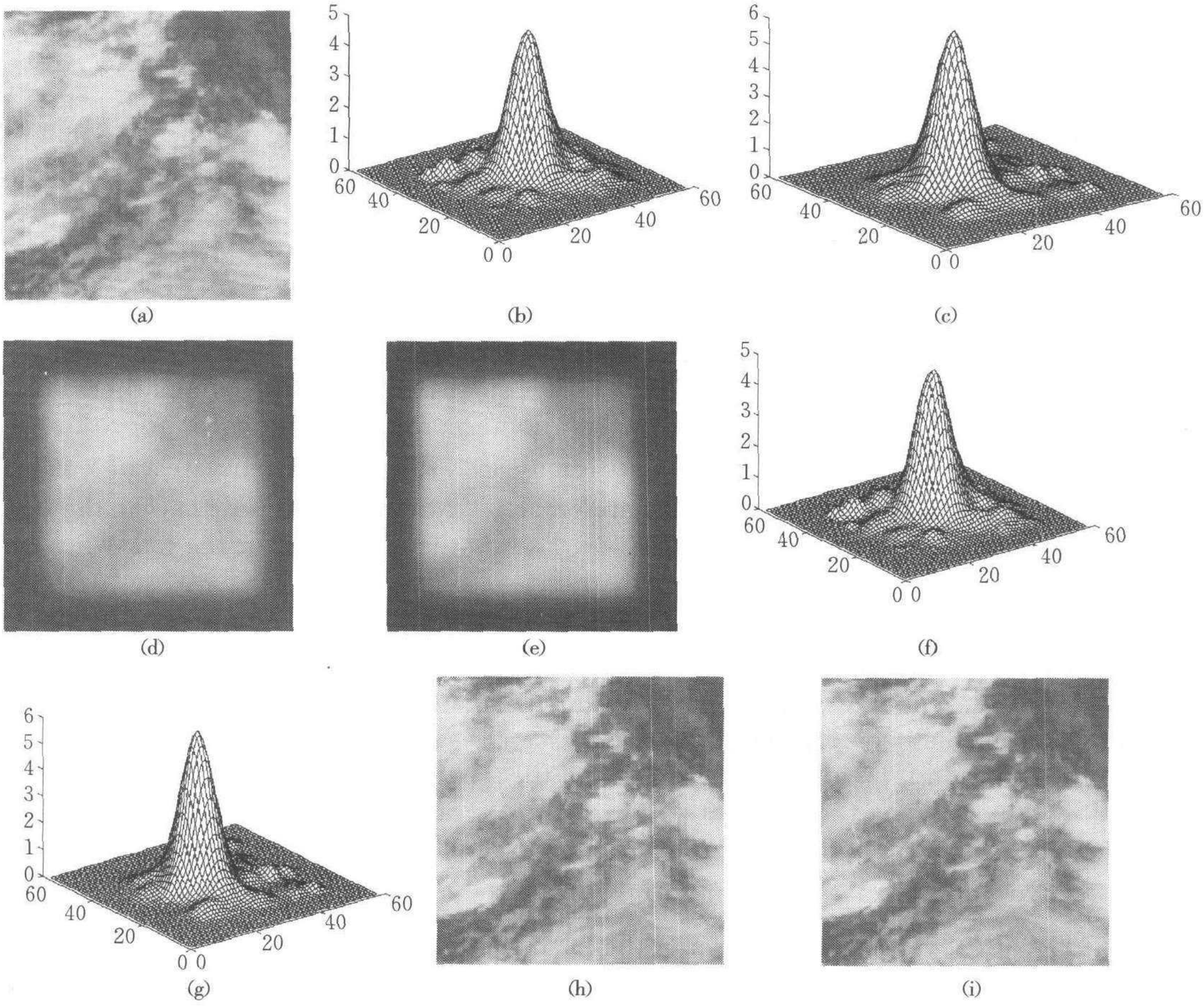

Fig. 2 (a) original image in size of 130×130; (b) and (c) two original PSFs; (d) and (e) two turbulence-degraded images; (f) and (g) two estimated PSFs, respectively; (h) and (i) two images restored from (d) and (c)

The two turbulence-degraded images are shown in Figs. 2(d) and 2(e). The PSFs estimated by using the direct method from the degraded images Figs. 2(d) and 2(e) are shown in Figs. 2(f) and 2(g), which are basically in agreement with the original PSFs. The two images restored from the two degraded images 2(d) and 2(e) are shown in Figs. 2(h) and 2(i), respectively. The good restoring effect shows that in absence of noise or very little noise, the direct method can restore image exactly.

The direct method is rather sensitive to noise, which will be illustrated with experiments. Fig. 3(a) shows the original image, of 120×120 pixels in size. Two frames of images as shown in Figs. 3(d) and 3(e) are restored from two frames of degraded image 3(b) and 3(c) without adding noise. Two images restored from two turbulence-degraded images 3(b) and 3(c) to which stochastic Gaussian white noise is added are shown in Figs. 3(f) and 3(g) with an SNR of 50db. With an increase of noise, the restoring effect becomes poorer and poorer.

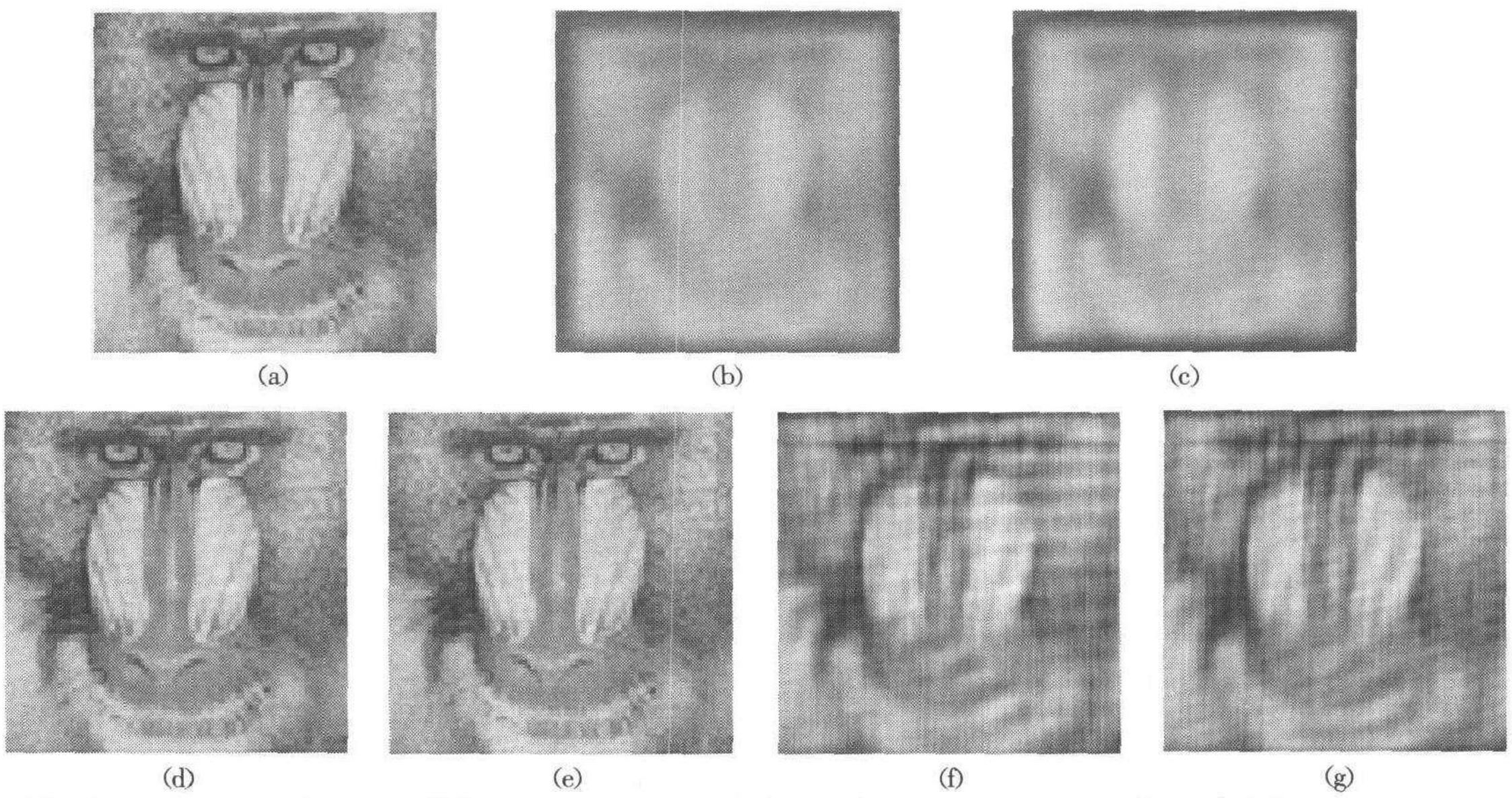

Fig. 3 (a) original image; (b) and (c) two turbulence-degraded images; (d) and (e) two restored images without noise; (f) and (g) two restored images with white noise added and with SNR 50dB

Below we shall verify the effect of restoration and the reliability of the optimization algorithm in the presence of noise. We shall still take Fig. 3(a) as the original image. The two frames of turbulence-degraded image are shown in Figs. 4(a) and 4(b). The excited zone of the PSF is 8×8 and with white noise added and an SNR of 30 dB. Figs. 4(c) and 4(d) are two image restored from Figs. 4(a) and 4(b). The time spent is 6 sec and the restoring effect is fairly ideal. With Frieden's method, two restored images are shown in Figs. 4(e) and 4(f). The time spent is 14 minutes and 42 seconds and there exist rather many false contours.

When blurring is increased and the excited zone of PSFs is expanded to 13×13, two turbulence-degraded images are generated. Add additive Gaussian noise of 40 dB and we have images as shown in Figs. 5 (a) and 5(b). Having them restored with the optimization algorithm we have the images shown in Figs. 5(c) and 5(d). The time spent is 3 minutes and 25 seconds. It can be seen from the results of the experiments that when there exist both blurring and rather loud noise, the optimization algorithm proposed is much better than Frieden's method in terms of the restoring effect as it has greatly reduced the degree of blurring, considerably reduced the false contours, and overcome the interference of

noise, proving the reliability of the proposed algorithm.

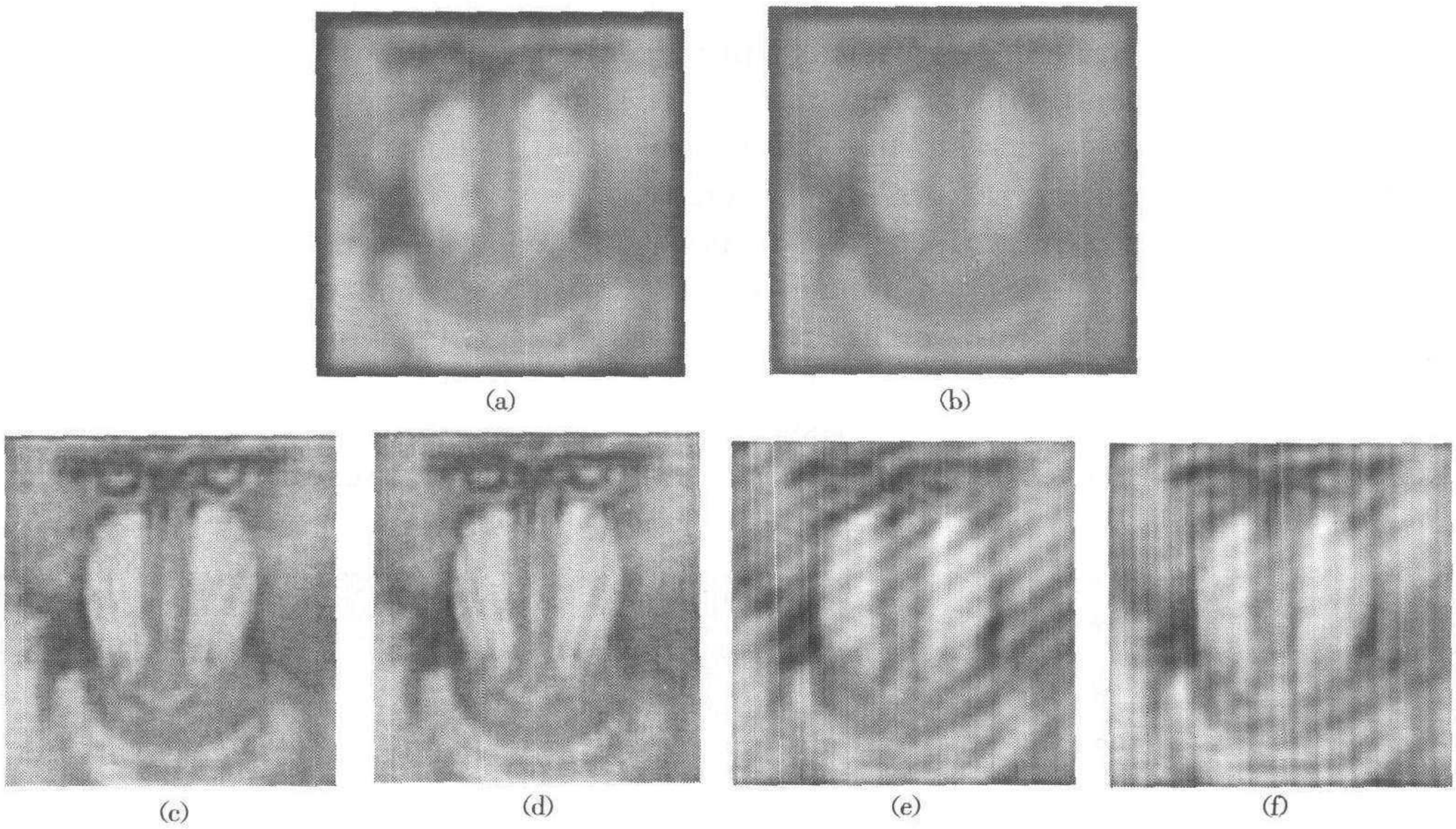

Fig. 4 (a) and (b) two turbulence-degraded images (PSF being 8×8), white noise added, with SNR 30dB; (c) and (d) two restored images using the proposed method; (e) and (f) two restored images with Frieden method

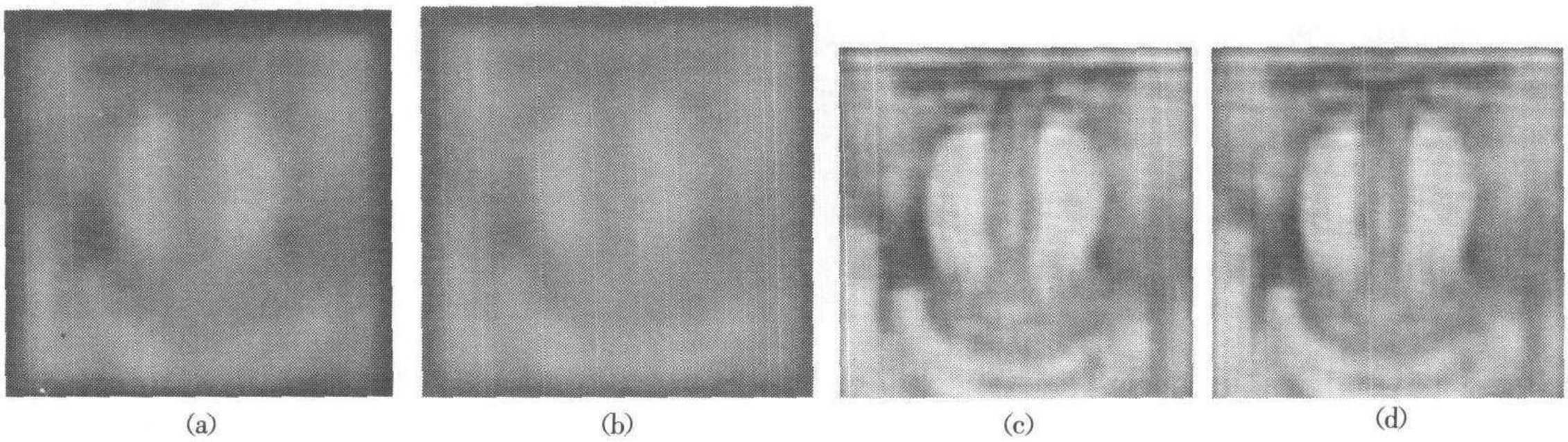

Fig. 5 (a) and (b) two turbulence-degraded images (PSF being 13×13), white noise added, with SNR 40dB; (c) and (d) two images restored using the proposed method

5 Conclusions

A new algorithm for restoring turbulence-degraded images is proposed and experimented on by directly estimating the turbulence PSF values with two turbulence-degraded images. This algorithm has helped to avoid the practice of measuring the PSF values by making use of available natural or artificial guide star. Comparisons with existing methods for restoring turbulence-degraded images show that the method is faster and fairly effective. However, when turbulence is rather strong, the turbulence-degraded images would be extremely blurred. Although the PSF values can be accurately and quickly calculated by using the direct method, its requirement on SNR is rather high. The optimization estimation method is found to overcome the interference with noise, but it takes too much time. Hence, in order to reduce the calculating workload and consumption of time, in the future work, we intend to adopt the multi-resolution technique based on wavelet transform to restore turbulence-degraded images.

References

1 Labeyrie A. Attainment of diffraction limited resolution in large telescopes by Fourier analyzing speckle patterns in star images. *Astronomy and Astrophysics*, 1970, **6**:85~87

2 Fondanella J C, Seve A. Reconstruction of turbulence-degraded images using the Knox-Thompson algorithm. *Journal of the Optical Society of America A*, 1987, **4**(3): 438~448

3 Lohmann A W, Weigelt G, Wirnitzer B. Speckle masking in astronomy: Triple correlation theory and applications. *Applied Optics*, 1983, **22**(24):4028~4037

4 Ellerbroke B L, Rhoadarmer T A. Adaptive wavefront control algorithms for closed loop adaptive optics. *Mathematical and Computer Modeling*, 2001, **33**:145~158

5 Ayers G R, Dainty J C. Iterative blind deconvolution method and its applications. *Optics Letter*, 1988, **13**(7): 547~549

6 Law N F, Lane R G. Blind deconvolution using least squares minimization. *Optics Communication*, 1996, **128**:341~352

7 Schulz T J. Multiframe blind deconvolution of astronomical images. *Journal of the Optical Society of America A*, 1993, **10**(5):1064~1073

8 Lam E Y, Goodman J W. Iterative statistical approach to blind image deconvolution. *Journal of the Optical Society of America A*, 2000, **17**(7): 1177~1184

9 Frieden B R, Oh C. Turbulent image reconstruction from a superposition model. *Optics Communication*, 1993, **98**: 241~244

10 Nagy James G, Plemmons Robert J, Torgersen Todd C. Iterative image restoration using approximate inverse preconditioning. *IEEE Transactions on Image Processing*, 1996, **5**(7):1151~1162

11 Frieden B R. An exact linear solution to the problem of imaging through turbulence. *Optics Communication*, 1998, **150**:15~21

12 Andrews H C, Hunt B R. Digital Image Restoration. Englewood Cliffs, NJ: Prentice Hall, 1977

13 Cao Zhi-Hao. Numerical Linear Algebra. Shanghai: Shanghai Fudan University Press, 1995. 62~68 (in Chinese)

14 Zhang Yong-Ping, Zheng Nan-Ning, Zhao Rong-Chun. Algorithm for image restoration based on variation and its convergence. *Acta Automatica Sinica*, 2002, **28**(5):673~680 (in Chinese)

ZHANG Tian-Xu Received his master degree from Huazhong University of Science and Technology in 1981 and his doctor degree from Zhejiang University in 1989. He is a professor and director with the State Key Laboratory of Image Processing and Intelligent Control. His research interests include automation target recognition, computer vision, precise missile guidance and image processing.

HONG Han-Yu Received his master degree from Taiyuan University of Science and Technology in 1991. He is an associate-professor and doctor candidate in the Institute of Pattern Recognition and Artificial Intelligence, Huazhong University of Science and Technology. His research interests include restoration of turbulence-degraded images, aero-optics, image processing, pattern recognition and computer graphics.

SUN Xiang-Hua Postgraduate student. Her research interests include signal and image processing.

SONG Zhi Postgraduate student. His research interests include aero-optics and image restoration.

基于估计点扩展函数值的湍流退化图像复原

张天序　　洪汉玉　　孙向华　　宋　治

(华中科技大学图像识别与人工智能研究所，图像信息处理与智能控制教育部重点实验室　武汉　430074)

(E-mail: txzhang@mail.hust.edu.cn, honghany@public.wh.hb.cn)

摘　要　提出了一种直接从湍流退化图像中估计湍流点扩展函数值的方法.本方法不再利用自然或人工向导星图像来测定点扩展函数，而是直接利用两帧连续短曝光湍流退化图像作为输入，在空域中对其进行适当的延拓，在频域中建立和选择关于湍流点扩展函数离散值的一系列计算方程.为了克服噪声的干扰，在点扩展函数的非负性和空间光滑性的约束条件下，将点扩展函数的计算问题转化为优化估计问题，通过极小化准则函数估计点扩展函数值，进而恢复退化图像.实验结果表明，本文方法十分有效，复原效果好.

关键词　图像复原，大气湍流，点扩展函数，空间相关性，优化估计

中图分类号　TP391